Research Article | Vol. 29, No. 22 / 25 Oct 2021 / Optics Express 34962
Optics EXPRESS

Piezo-modulated active grating for selecting X-ray pulses separated by one nanosecond

S. VADILONGA,[1,5,*] I. ZIZAK,[1,5] D. ROSHCHUPKIN,[2] E. EMELIN,[2] W. LEITENBERGER,[3] M. RÖSSLE,[1] AND A. ERKO[4]

[1]Helmholtz-Zentrum Berlin, Albert Einstein Str. 15, 12489 Berlin, Germany
[2]Institute of Microelectronics Technology and High Purity Materials Russian Academy of Sciences, 6 Academician Ossipyan Str., Chernogolovka, Moscow Region 142432, Russia
[3]Institut für Physik und Astronomie, Universität Potsdam, Karl-Liebknecht-Strasse 24-25, 14476 Potsdam, Germany
[4]Institut für angewandte Photonik e.V., Rudower Chaussee 29/31, 12489 Berlin, Germany
[5]Both authors contributed equally to this work
[*]simone.vadilonga@helmholtz-berlin.de

Abstract: We present a novel method of temporal modulation of X-ray radiation for time resolved experiments. To control the intensity of the X-ray beam, the Bragg reflection of a piezoelectric crystal is modified using comb-shaped electrodes deposited on the crystal surface. Voltage applied to the electrodes induces a periodic deformation of the crystal that acts as a diffraction grating, splitting the original Bragg reflection into several satellites. A pulse of X-rays can be created by rapidly switching the voltage on and off. In our prototype device the duty cycle was limited to ~1 ns by the driving electronics. The prototype can be used to generate X-ray pulses from a continuous source. It can also be electrically correlated to a synchrotron light source and be activated to transmit only selected synchrotron pulses. Since the device operates in a non-resonant mode, different activation patterns and pulse durations can be achieved.

1. Introduction

Recent interests in (ultra)fast X-ray processes have triggered new frontiers in X-ray science [1]. Time resolved experiments investigate non-equilibrium states, for example during chemical reactions [2,3], the transient structural response as result of a ultrashort laser excitation [4] and phonon dynamics driven by longitudinal acoustic phonons [5,6], the magnetization dynamics [7], thermal transport [8], and ferroelectric switching dynamics [9]. The change of the domain structure by the movement of domain walls of ferroelectric samples has been investigated with time-resolved X-ray diffraction [10]. To study the temporal dependency of the process, the action in the sample is triggered by a pumping signal, and measured at different time delays using the X-ray probe. Processes on a slower scale than several seconds can be studied by a continuous measurement after the excitation. As a pumping signal, different types of excitation can be used, e.g. laser pulses, electric or magnetic field pulses or similar. On shorter scales, the intensity of the probing signal is too low to provide a good statistics after just one measurement. However, if the process is reversible, this shortcoming can be solved by continuously triggering the process, and waiting to relax between two consequent excitations. The probe measures only once at a certain delay from the pumping pulse and the process is repeated for different delays until the sufficient statistics at all interesting delay times is acquired. The time resolution here is limited only by the duration of the pumping and probing pulses [11]. Therefore, the acquisition electronics does not need high time resolution. Except for the pulse duration, important parameter for these

#438570 https://doi.org/10.1364/OE.438570
Journal © 2021 Received 2 Aug 2021; revised 2 Sep 2021; accepted 2 Sep 2021; published 11 Oct 2021

Optics EXPRESS

experiments is the repetition rate of the experiment, which should not be shorter that the time the system requires to relax into the original state.

A useful property of the synchrotron radiation is, beside the unprecedented stability, brilliance and coherence, that the electrons are circulating in the storage ring in bunches, which inherently produce pulses of radiation [1]. In the third generation of synchrotron sources, the duration of the emitted X-ray pulses is on the 100 ps timescale, the repetition rate is in the order of several nanoseconds. Both these parameters depend on the construction properties of the light source. Efforts are made to modify these parameters for different experiments, to match them to the time scales of the studied process.

By alternating the momentum compaction factor (alpha) of the electron orbits in the storage ring, it is possible to shorten the pulses down to 5 ps. The so-called low-α mode is currently offered at most synchrotron light sources around the world [12–14]. Since the injection effectivity is much lower for shorter pulses, this is not suitable for a standard mode of the operation of the synchrotron light sources. Additionally, some insertion devices influence the length of the electron bunch, and have to be switched off in this mode of operation. A femtosecond short laser pulse is used to increase the momentum of a short slice of the electron bunch, sending them to a path slightly offset from the rest of the bunch. The beamline is aligned to accept only the radiation from the altered path, effecting in femtosecond x-Ray pulses [15–17].

Repetition rate can be modified on different stages of the light generation. The most frequent method is the alteration of the filling pattern of the storage ring. Most synchrotron light sources implement "multibunch" mode, where several hundred electron bunches orbit in the ring, and "single bunch" mode, where only one bunch is circulating, or variations of these, designated as "hybrid mode". Repetition rate can also be made slower than the ring period by sending electron bunches to an orbit which closes only after several revolutions around the ring [18–20]. Ultimately, the repetition rate of any kind of pattern is a function of the storage ring circumference. Another disadvantage is that all experiments at the storage ring receive the same bunch pattern.

For the reduction of the repetition rate at a specific experiment, it is more convenient to modulate the X-ray beam instead of the electrons in the storage ring. Different technical implementations exist or have been proposed. The most straight-forward approach is a chopper wheel rotating at high speed. At the rim of the rotating wheel, many small slits are mounted. The rotation of the wheel is correlated to the storage ring, so that the radiation from only one selected bunch passes through the slit, and the res is absorbed. The chopper used at BESSY II rotates with the frequency of 1 kHz and has slits at the rim [21]. Similar solutions were developed at SPring-8, at Petra III and at the ESRF synchrotron radiation facilities [22–25]. In the last few years, microelectromechanical systems (MEMS)-based x-ray optics were proposed as an alternative method to manipulate x-ray beams [26–30]. A fast vibrating Si-monocrystal is Bragg-diffracting only when the orientation is matching the Bragg condition. Both these methods are synchronized to the synchrotron frequency and select typically only the emitted X-ray pulse from the same designated electron bunch of the filling pattern of the storage ring. Furthermore, the construction and mechanical properties are tuned for one special pattern for a specific storage ring. While MEMS can select any bunch in multibunch mode, the filling pattern for the mechanical chopper must be modified by leaving a gap of about 100 ns before and after the selected bunch. Recently, the temporal shortening of an x-ray pulse using a photoacoustic Bragg switch has been published [31,32]. Tucoulou et al. employed surface acoustic waves excited on a crystal surface to pick a single pulse in the middle of a gap of 1.8 µs [33]. We have previously reported a pulse picker based on this method but operating in a different geometry that is able to discriminate pulses that are separated by at least 120 ns [34].

These methods are fundamentally limited by the beam size they can accept. The mass and the size of the MEMS device determine its resonant frequency, which is tuned to the circumference

Optics EXPRESS

of the storage ring. In case of the chopper wheel and of the surface acoustic wave pulse picker the accepted beam size is inversely proportional to the time resolution that can be achieved.

In this work we report the first experiments of a new method for selecting single x-ray pulses that are separated by 2 ns [35]. Therefore, comb-shaped metal electrodes with opposite polarity were deposited on single-crystalline lithium niobate, $LiNbO_3$, and langasite, $La_3Ga_5SiO_{14}$, both materials with excellent piezoelectric properties. When an external voltage is applied to these electrodes, the material below the electrodes expands and respectively compresses due to the converse piezoelectric effect. The result is a modulation of the crystal that creates a periodic modulation of the crystal surface and few unit cells below that acts as a diffraction grating for X-rays. The deformation forms on a sub-nanosecond timescale so that these devices can be used to switch on the grating only when X-ray pulses arrive at the pulse picker, which are then reflected and can be used for a time-resolved experiment. An aperture after the device is used to block the not-diffracted X-ray pulses when no voltage is applied, which generates a constant background. We experimentally verify that the synchronized activation of the grating with the incoming X-ray pulses can be used to select single X-ray pulses that are separated by 2 ns.

2. Methods and materials

2.1. Description and production of the samples

We report results from two different samples: the first sample has been produced on a 128 Y′-cut of black lithium niobate substrate, polished to 5 Å surface roughness. Black lithium niobate, compared to the normal lithium niobate, has a lower electrical resistivity (higher electrical conductivity) [36] that avoids the charge accumulation in the sample while still preserving the piezoelectric properties. Comb-shaped aluminium electrodes were deposited on the surface by vapor deposition by JSC Avangarde. The second sample was produced at the Institute of Microelectronics Technology and High Purity Materials, using an XY-cut of a langasite single crystal as a substrate, also polished to 5 Å surface roughness and comb-shaped aluminium electrodes were deposited on the surface by magnetron sputtering. In Fig. 1 we show schematically the structure of the deposited electrodes and in Table 1 we summarize the dimensions of the electrodes used in this work.

Table 1. Dimensions of the comb-shaped electrodes of the two investigated samples.

Sample	Substrate	Grating Period P_G	Electr. Period P_{AL}	Finger Width	Gap Width	Electr. Aperture	Electr. Length
LNB	$LiNbO_3$	4 μm	2 μm	1 μm	1 μm	200 μm	1.2 mm
LGS	$La_3Ga_5SiO_{14}$	2.8 μm	1.4 μm	0.7 μm	0.7 μm	200 μm	1.2 mm

2.2. Principle of the pulse picking device

We first discuss the working principle of the proposed pulse picking device. The single crystalline piezolectric optical element is oriented in a geometry close to the Bragg reflection. By temporary creating a grating on the surface of the crystal, the Bragg reflection splits into several satellites. Since the crystal is tilted from the Bragg condition, the diffraction appears only when the Bragg reflection is split, i.e. when the grating is activated. In a non-activated state the Bragg condition is given by the expression:

$$m\lambda = 2d \sin(\theta_B), \tag{1}$$

Optics EXPRESS

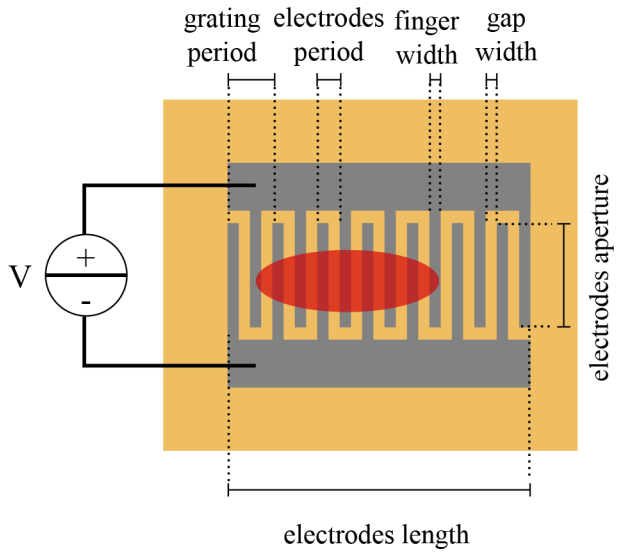

Fig. 1. Schematic of the samples used for the realization of the. X-ray pulse picking device: The piezoelectric substrate is in yellow, the Al electrodes in light grey, and the X-ray beam footprint in red. The picture is not to scale and the dimensions are summarized for both samples in Tab. 1.

where m is the diffraction order, λ is the wavelength of the incident radiation, d is the lattice spacing of the diffracting crystal planes, and θ_B the incident angle of the radiation on the diffraction planes for constructive interference.

To generate the grating at the surface, thin Al comb-shaped electrodes are deposited on the surface. The electrodes themselves are very thin ($\sim$ 100 nm), but they nevertheless act as a grating with the period P_{Al}. This is a parasitic effect that we tend to minimize. If the electrodes are alternately connected to a different electric potential, the electric field from positive and negative electrodes generates opposite strains in the piezoelectric crystal due to the converse piezoelectric effect. The surface of the crystal lowers or raises below the electrodes of the different potential. In our experiments, we had significant results with single-crystalline lithium niobate, $LiNbO_3$, and langasite, $La_3Ga_5SiO_{14}$. The Bragg-reflected signal from the regions of different heights is going to have a relative phase shift, so the distorted surface acts as a phase grating with the period $P_{\mathrm{G}} = P_{\mathrm{Al}}/2$. Both the Al and the phase grating split the Bragg intensity into to the satellites separated by [37]

$$\delta\theta \propto \frac{d}{P}, \tag{2}$$

from the Bragg reflection. Here P stands for either P_{Al} or P_{G}. Since the period of the aluminum grating P_{Al} is half of the diffraction grating period P_{G}, all even order diffraction satellites have an additional contribution from the diffraction from the Al electrodes. A small aperture around the exit beam improves the signal-to-noise ratio. The electrode arrays do not have to be straight, they can be shaped into zone plates, and the period may vary along the structure creating additional focusing effects.

The size of the optical element does not limit the reaction time, since there is no time needed to spread the deformation across the optical element. The deformation forms on a sub-nanosecond timescale so that these devices can be used to switch on the grating only when an X-ray pulse arrives at the pulse picker, which is then reflected and can be used for a time-resolved experiment. However, the activation of the diffraction grating for the selection of X-ray pulses requires

Optics EXPRESS

electronic equipment, which can be synchronized to a reference frequency derived from the storage ring or accelerator of the electron bunches at the synchrotron light source. See section 3.3 for a description of the grating activation circuits. We experimentally verify that the synchronized activation of the grating with the incoming X-ray pulses can be used to select single X-ray pulses that are separated by 2 ns.

3. Experimental setup

3.1. Time structure of BESSY II

The measurements presented in this article were performed at the BESSY II synchrotron radiation facility in Berlin, Germany. BESSY II is operated most of the time in the so-called "hybrid mode" in top-up operation where the number of the circulating charges is kept constant and, if necessary, charges are refilled. BESSY II operates at an electron energy of 1.7 GeV at 1.25 MHz repetition rate that is given by the circumference of the storage ring. This yields in total 400 bunches with 2 ns separation that can store electrons or are kept empty. The filling pattern in hybrid mode, see Fig. 2, offers an isolated bunch, the so-called single or camshaft bunch, whose charge corresponds to 4 mA and is in the center of a 200 ns wide gap followed by another isolated bunch of transverse excitation corresponding to 3 mA. Altogether 302 of the 400 available bins are filled and form the multibunch train with ~1 mA charge equivalent. Three additional "slicing" bunches are added on top of the multibunch train [38].

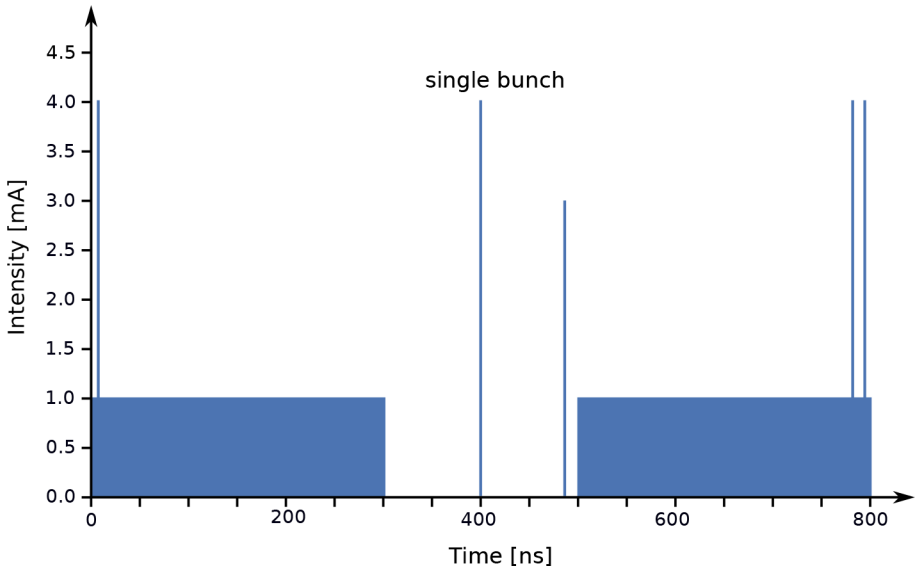

Fig. 2. Hybrid mode fill pattern at BESSY II at the time of the experiment.

3.2. XPP-KMC3 beamline at BESSYII

The pulse picking device was investigated at the XPP-KMC3 beamline at BESSY II [39]. A schematic view of the beamline is shown in Fig. 3. The double crystal monochromator is equipped with two Si 111 crystals and the energy used for the experiments was set to 8 keV, with an energy resolution of $E/\Delta E = 4500$. The sample was mounted on a four circle goniometer equipped with three translation axes. The X-ray beam is focused with a multilayer X-ray mirror to $150 \times 400\ \mu m^2$ at the sample position and the footprint has been further reduced using a circular Pt pinhole with 100 μm diameter positioned 10 cm before the sample. This ensured that the

Optics EXPRESS

X-ray beam footprint was smaller than the active area of the electrodes so they were overlapped as indicated in Fig. 1. For the presented experiments two different detectors have been used and both have been mounted ~50 cm behind the sample. The first detector is a scintillation detector (Cyberstar X2000, FMB Oxford) equipped with motorized horizontal aperture. The second detector used is a fast scintillator (Scionix) with an effective conversion efficiency of 10 photons/keV and a decay time of approximately 1 ns attached to a commercial photomultiplier assembly (PicoQuant PMA). All the time-resolved measurements of the samples were done in the Bragg diffraction geometry where the detector was set to 2θ with θ being the incidence angle of the X-rays onto the diffraction planes. For the LNB sample the 104 reflection at $\theta_B = 16.45°$ was used while for the LGS sample the 020 reflection at $\theta_B = 12.55°$ was investigated.

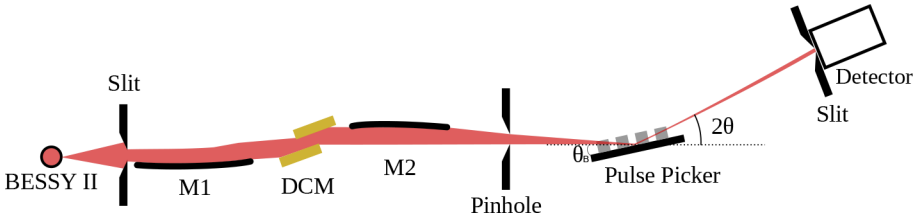

Fig. 3. Optical layout (side view) of the experiment at the XPP-KMC3 beamline at BESSY II. The picture is not to scale.

3.3. *Grating activation circuits*

Our aim is to use readily available electronics for the standard operation of the pulse picking device. To activate the grating, three different electronic circuits were used. The first circuit was used for the static characterization of the voltage response of the LNB sample. The sample electrodes were connected to a DC power supply (ES300, DeltaElektronika) and the applied voltage was varied between 0 – 10 V. The sample was rotated around the θ axis, a geometry often referred to as "rocking curve". The second circuit was used for the experiments with an effective time-resolution of 5 ns. The sample was connected to the output of a pulse and delay generator (DG645, Stanford Research System) that was synchronized to the 1.25 MHz timing signal of the storage ring of BESSY II and indicates the occurrence of one of the 400 bunches in the storage ring. The delay generator produces electrical voltage pulses as short as 2 ns with an output voltage of 5 V. The pulses have a rise and fall time of ~ 2 ns, hence the pulse does not reach the desired voltage of 5 V for pulses shorter than ~5 ns. The third circuit was used in order to be able to distinguish the different X-ray pulses that are only 2 ns apart, the signal of the delay generator was fed to an ultra-fast SiGe voltage comparator (ADCMP580, Analog Devices) that has a state transition time of 0.3 ns. Since the voltage comparator generates an output signal of only 0.4 V, it had to be amplified, which was achieved by connecting the output to a wide-band radio-frequency amplifier with 5 W power (KAW1020, AR Modular RF) connected to the sample electrodes.

4. Results

In the first part of the measurement, the crystal was rocked around the Bragg reflection while keeping the grating activation constant, to study the intensity of the satellites for different static conditions. In the second part, the activation of the grating was modulated to measure the time resolution and the stability of the device across several hours.

Static measurements The symmetric 104 reflection of LNB was aligned and the intensity of the reflected intensity of this Bragg reflection was measured to be approximately 68% of the incident x-ray beam. Rocking curves were recorded for different voltages applied to the electrodes,

Optics EXPRESS

as shown in Fig. 4. We observe that as the voltage is applied and increased, diffraction satellites at both sides of the Bragg reflection appear, as expected. The amplitude of the deformation depends on the applied voltage as given by the converse piezoelectric effect. At voltages larger than 3 V, higher interference maxima can be observed and at 10 V the ±4 order is clearly visible. The intensity of the first diffraction satellite reaches the maximum for a voltage of 9 V whereas there is still a noticeable increase between 9 V and 10 V for higher diffraction orders.The highest efficiency of the pulse picker is achieved by using the m=-1 diffraction order, that has an intensity of approximately 50% of the Bragg peak, that accounts for ~ 34% of the direct beam intensity.

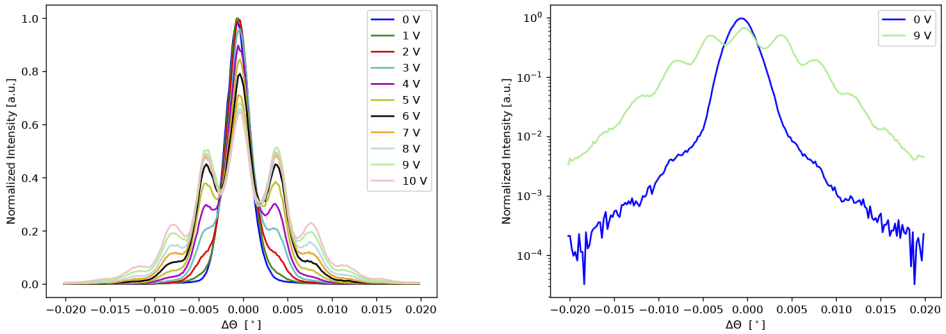

Fig. 4. Left: rocking curves around the Bragg peak of LNB for different excitation voltages, normalized to the measurement at 0 V. ΔΘ is the deviation from the Bragg angle. **Right**: rocking curves for the grating excitation voltage of 0 V and 9 V, in logarithmic scale. This illustrates that the satellites and the accompanying background on both sides of the Bragg reflection relatively gain intensity as the voltage increases, especially for the tilt angle matching the $m = \pm 1$ satellite.

Time-resolved measurements In the following, we investigate the isolated single bunch of the BESSY II hybrid mode filling pattern for the characterization of the pulse picking device characteristics. The selected electron bunch is separated by 50 ns from other bunches, giving us the opportunity to study the resolution of the switching device. As a trigger for the grating activation, the so-called beam marker signal from the storage ring was used, and a variable delay was added to it. We expect that when the grating is activated during the clearing gap, a few photons are going to be reflected and low intensity is going to be measured by the detector. On the other hand, if the grating is activated when the photons from the selected bunch pulse reach the surface, the diffracted intensity should increase. In Fig. 5 we show measurements of the diffracted intensity of the $m = -1$ diffraction satellite for different duration of the grating activation as a function of the delay between the trigger signal and the activation of the grating. By varying the delay we can measure how fast the grating is activated, and how long it stays this way. For each delay, we measured a rocking curve. Intensities at the position of the $m = -1$ diffraction satellite were collected and plotted. For the 10 ns long grating activation period, the diffracted intensity shown by the blue-filled circles is highest, and the time-resolution given by the FWHM~9.9 ns of the peak essentially reflects the duration of the grating activation. For the activation duration of 5 ns FWHM~5.5 ns was measured, however, the reflected intensity was slightly reduced. For the duration of 2 ns the intensity was reduced to about 50%. Further reduction of the activation time was not possible, because the signal generator (DG645, Stanford Research System) had the transition time of 2 ns. A FWHM~2.7 ns was measured.

To provide an electric signal shorter than 2 ns, a special SiGe voltage comparator was used, however without the option to modify the pulse height, so that the amplitude is not to scale with other time resolution measurements. The single bunch was scanned in 0.1 ns increments using the $m = -2$ diffraction order. The result is shown in Fig. 6 by the blue filled symbols. We fit the

Optics EXPRESS

time trace with a linear combination of a Gaussian function and a linear function representing

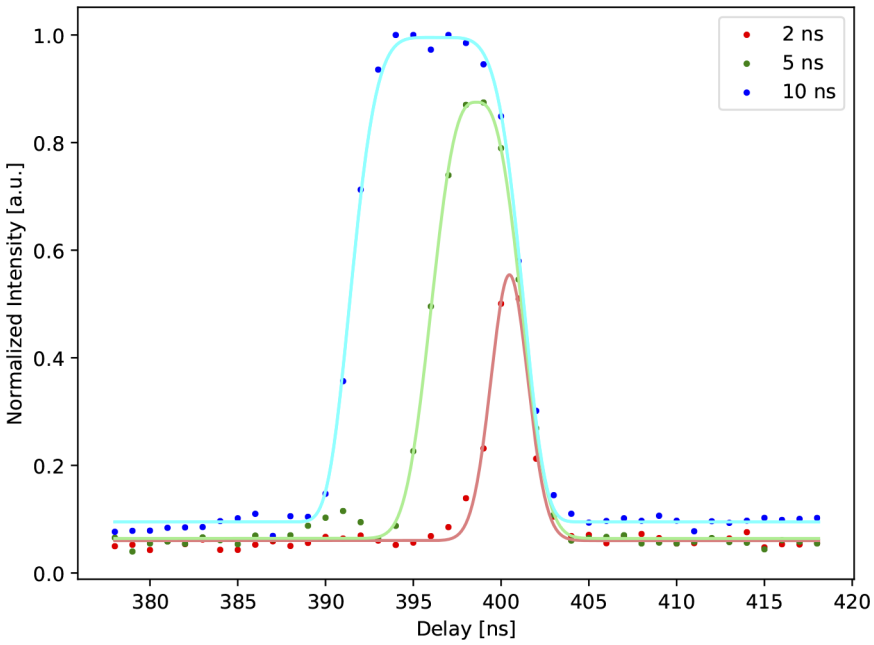

Fig. 5. Dependency of the reflected intensity on the delay time for the activation duration of 10 ns, 5 ns, and 2 ns. The experimental data are shown as filled dots and the lines are a guide for the eye. The delay-times refer to the fill pattern showed in Fig. 2.

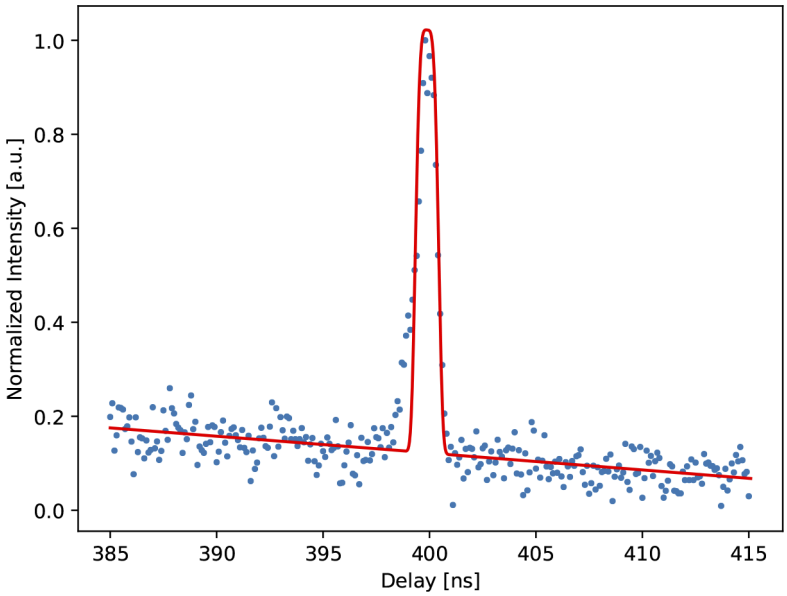

Fig. 6. Delay scans of the activation time t_0 of the grating with a duration of 1 ns. The experimental data are represented by the filled dots, the red solid line a the fit with a Gaussian line shape and additional linear background. The delay-times refer to the fill pattern showed in Fig. 2.

Optics EXPRESS

the background, which is shown in Fig. 6 as solid red line. The decreasing intensity background is attributed to the fact that the angle between incident radiation and the sample was slightly drifting during the measurements. The FWHM of the peak is 1.1 ns as expected for the activation of the grating with a pulse duration of 1 ns.

Since the measured time resolution was comparable with the delay in two bunches in a multibunch pattern (2 ns, we attempted separation of a single bunch from the multibunch pattern. In the following, we present data obtained activating the grating for 1 ns and sampling the multibunch train. The time delay between the synchronization signal from the storage ring and the grating activation was increased in 0.1 ns steps while still being tuned to the $m = -2$ diffraction order. As shown in Fig. 7, we can clearly separate the individual bunches. The measured diffracted intensity as a function of delay is shown by the filled blue symbols, the red solid line is a fit with three Gaussian functions that serve as guide-to-the-eye. For these measurements, the background level is higher than seen for the single bunch case presented in Fig. 6 before, because the electron bunches are densely packed and separated by only 2 ns, and the grating activation duration had a FWHM of 1 ns. In contrast, the isolated single bunch is surrounded by the clearing gap, which improves the signal-to-noise ratio drastically.

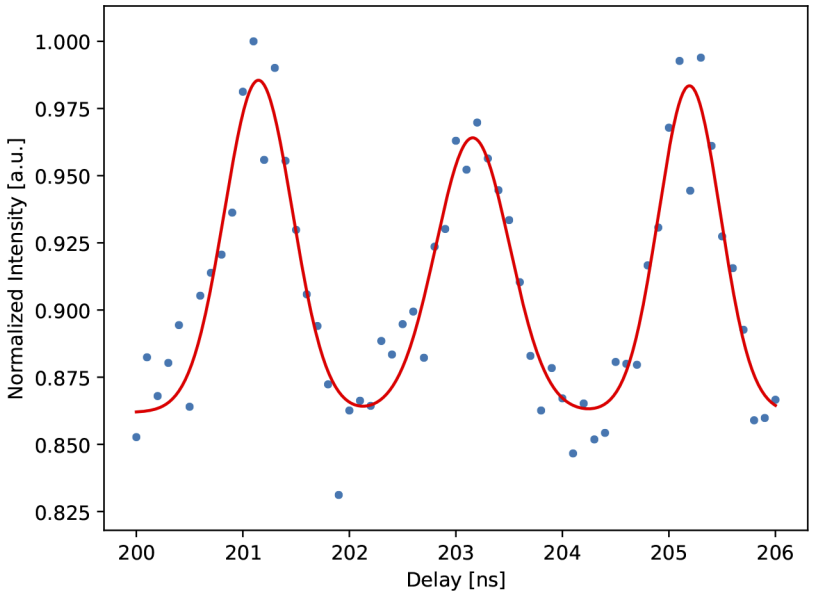

Fig. 7. Delay scan of the activation time t_0 of the grating with an activation duration of 1 ns where the grating is activated within the multibunch train. The experimental data represent the diffracted intensity and is shown as filled circles, the red line is a guide to the eye. The different bunches are clearly identified and they are separated by 2 ns. The delay-times refer to the fill pattern showed in Fig. 2.

The rejection ratio can be defined as the ratio of the diffracted intensity of the X-ray single bunch measured when the grating is activated with respect to the measured background generated by other 400 X-ray pulses when the grating is not activated. In Fig. 8 the rejection ratio for different angles, for a grating activation for 10 ns, is shown. In this figure, it is visible that the rejection ratio is higher for the negative diffraction orders. One also notes that the rejection ratio of the ±2 order diffraction order is roughly a factor of 2 larger than for the ±1 order. For higher X-ray photon flux, the ±1 order is preferable with a however slightly reduced rejection ratio. The best rejection ratio is obtained for the ±2 diffraction orders.

Optics EXPRESS

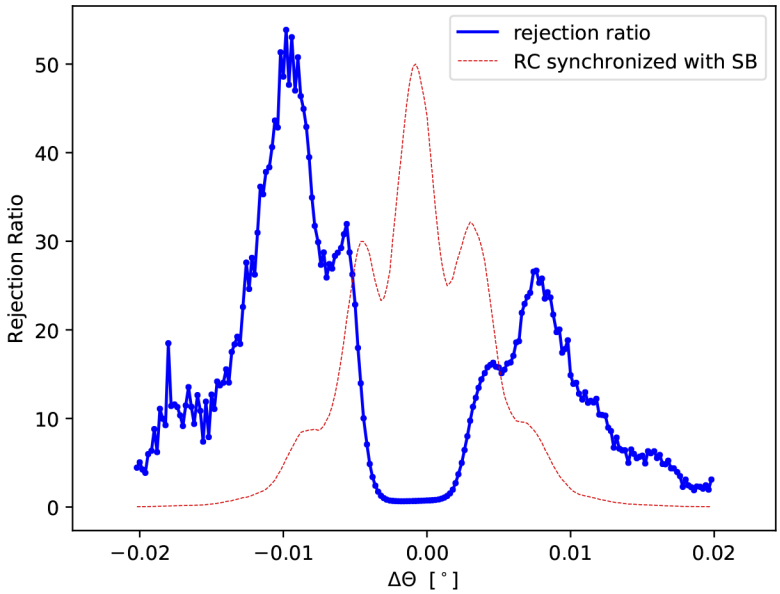

Fig. 8. In blue the rejection ratio as function of the deviation $\Delta\theta$ from the Bragg angle θ_B for an activation duration of the grating of 10 ns calculated from the rocking curves for time 395 ns and 370 ns. The red dotted line is a rocking curve obtained synchronizing the grating activation with the single bunch and serves as an indication of the position of the diffraction satellites.

Stability measurements The long-time stability of the LGS sample was carefully tested over several hours. The grating was a activated using the delay generator, with a grating activation

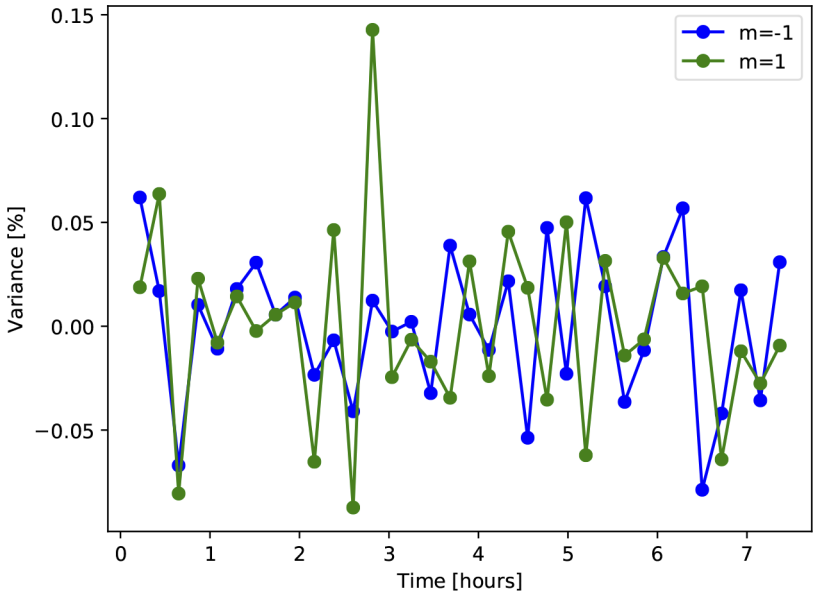

Fig. 9. Stability measurements: variance of the intensity of the m=±1 diffraction satellites vs time.

Optics EXPRESS

period of 20 ns. Every 15 minutes, a full rocking curve of the sample was measured and normalized to the maximum intensity of the Bragg reflection. In Fig. 9 we plot the variance of the intensity of the m=±1 diffraction satellite against time. The variance of the measured diffraction intensity of the first and second diffraction orders as function of time is better than ±0.5% over an extended period of 7 hours.

5. Discussion

We propose the design of a pulse picking device for hard X-ray radiation at synchrotron light sources. Our experiment characterize test devices at BESSY II during hybride mode operation where X-ray pulses are separated by 2 ns, that is, our device has a time-resolution of 1 ns. We use in our approach for the design and operation of the pulse picking device a simple setup that does not rely on high precision mechanical rotation and translation stages or high-speed electronics. Our device consists of a commercially available piezoelectric substrate with thermally evaporated metallic comb-shaped electrodes, which can easily be produced by established standard evaporation processes or similar coating techniques. The excitation of the grating relies on standard and at most synchrotrons readily available electronics.

At the XPP-KMC3 beamline at the BESSY II synchrotron light source, we have shown that it is possible to activate the diffraction grating quickly and reliably to extract the isolated X-ray single bunch, see Fig. 6. We note that on the left-hand side of each of the peaks in Fig. 5 a small structure is visible, which we attribute to a reflection of the electric signal due to the impedance mismatch between the electrodes, the cable, and the pulse generator. Of course, this parameter can be improved using a design of the comb-shaped electrodes that matches the impedance of the RF cables used, or a different pulse generator. However, we decided during the design process of the device that parameters like the total area covered of the active grating are more important for the daily operation of such a device at a synchrotron beamline, which will reduce the alignment and maintenance effort significantly. In this experimental work the active area of the device was 1.2×0.2 mm^2, and it can be further extended without loss of time-resolution.

The observed background in the measurements originates from the main Bragg reflection of the substrate. From the total 300 mA current circulating in the storage ring, the single bunch carries only 4 mA and thus the majority of the filling pattern contributes to the background, which mostly is produced by the multibunch train. Nevertheless, we obtain a rejection ratio of about 50 as can be seen in Fig. 8, even though during this experiment we did not apply the optimum voltage of 9 V for the excitation of the grating. This can be optimized with a different pulse generator.

In the introduction, we have discussed the processes that are important for the functionality of the device as a pulse picker. One of the main contributions to the noise comes from the electrodes that form the diffraction grating in the piezoelectric substrate. However, the electrodes themselves form an additional grating with twice the period of the grating generated by the externally applied electric field. This contribution could be reduced using a different geometry for the design of the electrodes. The so-called split geometry [40] could be used where two positive electrode fingers are followed by two negative electrode fingers. The period of the absorption grating would be one-quarter of the period of the diffraction grating and thus move the contribution of the absorption grating further away from the main diffraction grating response, i.e to the satellite $m = \pm 4$. The rejection ratio could be further improved using a smaller period of the grating, which would increase the angular separation of the diffraction satellites given by Eq. (2). Using thicker high-quality substrates reduces the Darwin width of the Bragg reflection, which in turn results in improved separation of the diffraction satellites and thus improves the rejection ratio as well.

Optics EXPRESS

We find from the statistical analysis of the diffracted intensity that the device efficiency is constant within a variation of ±0.5% over at least 7 hours. Comb-shaped electrodes are commonly used in the industry. Such structures also referred to as interdigital transducers, are well established and used for example to produce sensors and delay lines. These are proven to reliably work over many years [40,41]. Our experimental results give no indication of any beam degradation effects. Nevertheless, this cannot be excluded for longer time periods. It is important to note that the device is not designed to be exposed directly to a white or pink beam of a beamline but is intended to be placed downstream of a monochromator, as sketched in Fig. 3. The simple design ensures in the eventuality of severe device degradation the fast and cheap replacement of the pulse picker.

6. Comparison with other pulse picking methods

Several methods of the time structure manipulation of the X-ray signal are mentioned in the introduction. Each of these methods has its own strong and weak sides, rendering it more or less compatible with a specific experiment and experimental station. In the following section, we would like to emphasize the differences between the methods, as well as to point out the specific advantages of the novel method presented here.

The advantage of the rotating chopper wheels is that they work independently from the X-ray energy and its bandwidth [21]. However, the chopper wheel rotates in ultrahigh vacuum and is levitated on magnetic bearings, which requires a certain extended level of maintenance and infrastructure. Pulses at the kHz chopper installed at BESSY are picked by 1252 high-precision slits of 70 μm width placed on the outer rim of the wheel, which correspond to a temporal opening window of the chopper of 70 ns. This working principle guarantees an efficiency of 100% and an excellent rejection ratio of unwanted X-rays.

Contrary to rotating mechanical choppers, MEMS devices are tailored for a certain wavelength, hence require well-defined experimental conditions [28,29]. As the MEMS consists of a thin, single-crystalline piece of silicon, such devices diffract or transmit X-rays by changing their orientation relative to the incident X-ray beam. The mass of the MEMS structure is tuned such that its resonant frequency matches the storage ring frequency, and they managed to achieve a time resolution of 300 ps.

The SAW-based pulse picker proposed by Tucoulou *et al.* [33] works by generating an acoustic wave that propagates parallel to the surface of the crystalline substrate and acts as a diffraction grating for the illuminating x-rays. In this case, the time resolution is given by the time that is required from the surface acoustic wave to cross the X-ray beam footprint on the device. Changing the geometry from meridional to sagittal, which means that the X-ray beam crosses the X-ray footprint on the device in the transverse direction, we were able to improve the time resolution down to 120 ns [34]. Of course, this method relies on a monochromatic beam and an efficiency as high as 40% of the incoming X-ray beam intensity has been achieved [34].

In general, another limitation of most pulse picking devices arises from the maximum accepted beam-size. In the case of the rotating chopper wheel, it is limited by the size of the slits or channels in the outer part of the wheel. The aperture size can be reduced at the cost of the transmitted intensity as the channel will be closed before the full X-ray pulse will have passed through the groove. In MEMS devices the limitation originates from the finite area of the reflecting element: the mass of the reflector for MEMS system has to be chosen such that its oscillation frequency matches the revolution frequency of the electrons in the storage ring, which is in the MHz range, and thus requires tiny structures. In the case of the SAW-driven pulse pickers, the X-ray beam footprint limits the time resolution and efficiency.

Our new design combines a time resolution on the order of 1 ns with the flexibility to select X-ray pulses from the available time structure of the storage ring with a large beam diameter acceptance. Therefore this technique is also attractive for beamlines with lower X-ray flux

Optics EXPRESS

because this depends on the area covered by the comb-shaped electrodes, which can easily be increased up to several square millimeters. The device itself relies on motors only for alignment. For the pulse selection no moving parts are necessary, thus simplifies the required infrastructure and reduces the maintenance during the operation. Additionally, due to the grating activation mechanism, the method presented here is not limited to periodical pulse picking patterns but can generally be used for non periodical (arbitrary) selection patterns that are tailored to the needs of the experiment.

7. Conclusions

We reported for the first time the proposal and successful characterization of a simple and yet affordable method for temporal modulation of an X-ray beam. The modulation is achieved by modifying the Bragg reflection of a piezoelectric crystal by an electrode that induces a periodic deformation of the crystal surface that acts as a diffraction grating for X-rays. We show that in the present configuration its efficiency reaches up to 34% of the incoming beam intensity, and we experimentally demonstrate a time-resolution of 1 ns independent of the accepted beam size, and limited only by the driving electronics. The grating is activated using an electrical signal, and different activation patterns and pulse duration can be achieved without any hardware modification. This device could be used to generate X-ray pulses from a continuous source or to reduce the repetition rate of the synchrotron light source. By correlating the device to the storage ring, individual x-pulses can be selected. This can be implemented in a wide range of beamlines, and flexibly adapted to the needs of individual users.

Funding. Helmholtz-Zentrum Berlin für Materialien und Energie; Ministry of Science and Higher Education of the Russian Federation (075-00355-21-00).

Acknowledgments. The authors thank Helmholtz-Zentrum Berlin for the allocation of synchrotron beamtime at the XPP-KMC3 beamline. The authors thank JSC Avangard and in particular Dr. S. Dzyubanenko for his support and his efforts producing high-quality samples.

Disclosures. The authors declare no conflicts of interest.

Data availability. Data underlying the results presented in this paper are not publicly available at this time but may be obtained from the authors upon reasonable request.

References

1. R. Schoenlein, T. Elsaesser, K. Holldack, Z. Huang, H. Kapteyn, M. Murnane, and M. Woerner, "Recent advances in ultrafast x-ray sources," Philos. Trans. R. Soc., A **377**(2145), 20180384 (2019).
2. F. Zamponi, P. Rothhardt, J. Stingl, M. Woerner, and T. Elsaesser, "Ultrafast large-amplitude relocation of electronic charge in ionic crystals," Proc. Natl. Acad. Sci. U. S. A. **109**(14), 5207–5212 (2012).
3. J. Kim, K. H. Kim, K. Y. Oang, J. H. Lee, K. Hong, H. Cho, N. Huse, R. W. Schoenlein, T. K. Kim, and H. Ihee, "Tracking reaction dynamics in solution by pump-probe X-ray absorption spectroscopy and X-ray liquidography (solution scattering)," Chem. Commun. **52**(19), 3734–3749 (2016).
4. D. Schick, M. Herzog, A. Bojahr, W. Leitenberger, A. Hertwig, R. Shayduk, and M. Bargheer, "Ultrafast lattice response of photoexcited thin films studied by X-ray diffraction," Struct. Dyn. **1**(6), 064501 (2014).
5. R. Shayduk, M. Herzog, A. Bojahr, D. Schick, P. Gaal, W. Leitenberger, H. Navirian, M. Sander, J. Goldshteyn, I. Vrejoiu, and M. Bargheer, "Direct time-domain sampling of subterahertz coherent acoustic phonon spectra in $SrTiO_3$ using ultrafast x-ray diffraction," Phys. Rev. B **87**(18), 184301 (2013).
6. A. Bojahr, M. Gohlke, W. Leitenberger, J. Pudell, M. Reinhardt, A. von Reppert, M. Roessle, M. Sander, P. Gaal, and M. Bargheer, "Second Harmonic Generation of Nanoscale Phonon Wave Packets," Phys. Rev. Lett. **115**(19), 195502 (2015).
7. T. Tsuyama, S. Chakraverty, S. Macke, N. Pontius, C. Schüßler-Langeheine, H. Y. Hwang, Y. Tokura, and H. Wadati, "Photoinduced demagnetization and insulator-to-metal transition in ferromagnetic insulating $BaFeO_3$ thin films," Phys. Rev. Lett. **116**(25), 256402 (2016).
8. A. Koc, M. Reinhardt, A. von Reppert, M. Rössle, W. Leitenberger, K. Dumesnil, P. Gaal, F. Zamponi, and M. Bargheer, "Ultrafast x-ray diffraction thermometry measures the influence of spin excitations on the heat transport through nanolayers," Phys. Rev. B **96**(1), 014306 (2017).
9. C. Kwamen, M. Rössle, M. Reinhardt, W. Leitenberger, F. Zamponi, M. Alexe, and M. Bargheer, "Simultaneous dynamic characterization of charge and structural motion during ferroelectric switching," Phys. Rev. B **96**(13), 134105 (2017).

Optics EXPRESS

10. C. Kwamen, M. Rössle, W. Leitenberger, M. Alexe, and M. Bargheer, "Time-resolved X-ray diffraction study of the structural dynamics in an epitaxial ferroelectric thin $Pb(Zr_0.2Ti_0.8)O_3$ film induced by sub-coercive fields," Appl. Phys. Lett. **114**(16), 162907 (2019).
11. P. Ruello and V. E. Gusev, "Physical mechanisms of coherent acoustic phonons generation by ultrafast laser action," Ultrasonics **56**, 21–35 (2015).
12. K. Holldack, J. Bahrdt, A. Balzer, U. Bovensiepen, M. Brzhezinskaya, A. Erko, A. Eschenlohr, R. Follath, A. Firsov, W. Frentrup, L. Le Guyader, T. Kachel, P. Kuske, R. Mitzner, R. Müller, N. Pontius, T. Quast, I. Radu, J.-S. Schmidt, C. Schüßler-Langeheine, M. Sperling, C. Stamm, C. Trabant, and A. Föhlisch, "FemtoSpeX: a versatile optical pump–soft X-ray probe facility with 100fs X-ray pulses of variable polarization," J. Synchrotron Radiat. **21**(5), 1090–1104 (2014).
13. M. Labat, J.-B. Brubach, A. Ciavardini, M.-E. Couprie, E. Elkaim, P. Fertey, T. Ferte, P. Hollander, N. Hubert, E. Jal, C. Laulhé, J. Luning, O. Marcouillé, T. Moreno, P. Morin, F. Polack, P. Prigent, S. Ravy, J.-P. Ricaud, P. Roy, M. Silly, F. Sirotti, A. Taleb, M.-A. Tordeux, and A. Nadji, "Commissioning of a multi-beamline femtoslicing facility at SOLEIL," J. Synchrotron Radiat. **25**(2), 385–398 (2018).
14. G. Sciaini, "Recent advances in ultrafast structural techniques," Appl. Sci. **9**(7), 1427 (2019).
15. A. A. Zholents and M. S. Zolotorev, "Femtosecond x-ray pulses of synchrotron radiation," Phys. Rev. Lett. **76**(6), 912–915 (1996).
16. K. Holldack, R. Ovsyannikov, R. Mueller, M. Scheer, M. Gorgoi, D. Kuehn, T. Leitner, S. Svensson, N. Martensson, and A. Foelisch, "Single bunch x-ray pulses on demand from a multi-bunch synchrotron radiation source," Nat. Commun. **5**(1), 4010 (2014).
17. C. Sun, G. Portmann, M. Hertlein, J. Kirz, and D. S. Robin, "Pseudo-single-bunch with adjustable frequency: A new operation mode for synchrotron light sources," Phys. Rev. Lett. **109**(26), 264801 (2012).
18. P. Goslawski, A. Jankowiak, F. Kramer, M. Ries, M. Ruprecht, and G. Wuestefeld, "Transverse resonance island buckets as bunch separation scheme," *Proc. 8th Int. Particle Accelerator Conf. (IPAC'17)* pp. 3059–3062 (2017).
19. M. Ries, J. Feikes, T. Goetsch, P. Goslawski, J. Li, M. Ruprecht, A. Schälicke, and G. Wüstefeld, "Transverse resonance island buckets at the MLS and BESSY II," *Proc. 6th International Particle Accelerator Conference (IPAC'15)*, Richmond, VA, USA, May 3-8, 2015 pp. 138–140 (2015). Https://doi.org/10.18429/JACoW-IPAC2015-MOPWA021.
20. P. Goslawski, J. Feikes, K. Holldack, A. Jankowiak, R. Ovsyannikov, M. Ries, M. Ruprecht, A. Schaelicke, and G. Wuestefeld, "Resonance island experiments at bessy ii for user applications," *Proc. 7th Int. Particle Accelerator Conf. (IPAC'16)* pp. 3059–3062 (2016).
21. D. F. Förster, B. Lindenau, M. Leyendecker, F. Janssen, C. Winkler, F. O. Schumann, J. Kirschner, K. Holldack, and A. Föhlisch, "Phase-locked mhz pulse selector for x-ray sources," Opt. Lett. **40**(10), 2265–2268 (2015).
22. H. Osawa, T. Kudo, and S. Kimura, "Development of high-repetition-rate x-ray chopper system for time-resolved measurements with synchrotron radiation," Jpn. J. Appl. Phys. **56**(4), 048001 (2017).
23. H. Osawa, T. Ohkochi, M. Fujisawa, S. Kimura, and T. Kinoshita, "Development of optical choppers for time-resolved measurements at soft X-ray synchrotron radiation beamlines," J. Synchrotron Radiat. **24**(3), 560–565 (2017).
24. S. Kuechemann, C. Mahn, and K. Samwer, "Note: Significant increase to the temporal resolution of 2d x-ray detectors using a novel beam chopper system," Rev. Sci. Instrum. **85**(1), 016105 (2014).
25. M. Cammarata, L. Eybert, F. Ewald, W. Reichenbach, M. Wulff, P. Anfinrud, F. Schotte, A. Plech, Q. Kong, M. Lorenc, B. Lindenau, J. Räbiger, and S. Polachowski, "Chopper system for time resolved experiments with synchrotron radiation," Rev. Sci. Instrum. **80**(1), 015101 (2009).
26. A. Siria, O. Dhez, W. Schwartz, G. Torricelli, F. Comin, and J. Chevrier, "A MEMS-based high frequency x-ray chopper," Nanotechnology **20**(17), 175501 (2009).
27. I. W. Jung, Z. Li, Y. Gao, D. Walko, J. Wang, G. Shenoy, and D. Lopez, "High repetition-rate x-ray pulse selection at synchrotron sources," in *2016 International Conference on Optical MEMS and Nanophotonics (OMN)*, (2016), pp. 1–2.
28. P. Chen, D. A. Walko, I. W. Jung, Z. Li, Y. Gao, G. K. Shenoy, D. Lopez, and J. Wang, "Application of mems-based x-ray optics as tuneable nanosecond choppers," Adv. X-Ray/EUV Opt. Components XII **10386**, 103860M (2017).
29. P. Chen, I. W. Jung, D. A. Walko, Z. Li, Y. Gao, G. K. Shenoy, D. López, and J. Wang, "Ultrafast photonic micro-systems to manipulate hard x-rays at 300 picoseconds," Nat. Commun. **10**(1), 1158 (2019).
30. P. Chen, I. W. Jung, D. A. Walko, Z. Li, Y. Gao, T. Mooney, G. K. Shenoy, D. Lopez, and J. Wang, "Optics-on-a-chip for ultrafast manipulation of 350-mhz hard x-ray pulses," Opt. Express **29**(9), 13624–13640 (2021).
31. M. Sander, A. Koc, C. T. Kwamen, H. Michaels, A. v. Reppert, J. Pudell, F. Zamponi, M. Bargheer, J. Sellmann, J. Schwarzkopf, and P. Gaal, "Characterization of an ultrafast bragg-switch for shortening hard x-ray pulses," J. Appl. Phys. **120**(19), 193101 (2016).
32. M. Sander, R. Bauer, V. Kabanova, M. Levantino, M. Wulff, D. Pfuetzenreuter, J. Schwarzkopf, and P. Gaal, "Demonstration of a picosecond Bragg switch for hard X-rays in a synchrotron-based pump–probe experiment," J. Synchrotron Radiat. **26**(4), 1253–1259 (2019).
33. R. Tucoulou, D. Roschupkin, I. Schelokov, M. Brunel, L. Ortega, E. Ziegler, M. Lingham, C. Mouget, and S. Douillet, "High frequency electro-acoustic chopper for synchrotron radiation," Nucl. Instrum. Methods Phys. Res., Sect. B **132**(1), 207–213 (1997).
34. S. Vadilonga, I. Zizak, D. Roshchupkin, A. Petsiuk, I. Dolbnya, K. Sawhney, and A. Erko, "Pulse picker for synchrotron radiation driven by a surface acoustic wave," Opt. Lett. **42**(10), 1915–1918 (2017).

Optics EXPRESS

35. S. Vadilonga, I. Zizak, and A. Erko, "Anordnung und Verfahren zur Manipulation oder Erzeugung von Röntgenpulsen".
36. S. Jen and R. Bobkowski, "Black lithium niobate saw device fabrication and performance evaluation," 2000 IEEE Ultrason. Symp. Proceedings. An Int. Symp. (Cat. No.00CH37121) **1**, 269–273 (2000).
37. A. Erko, M. Idir, T. Krist, and A. G. Michette, *Modern Developments in X-Ray and Neutron Optics* (Springer, 2008).
38. "Machine status," https://www.helmholtz-berlin.de/forschung/oe/be/operation-accelerator/betriebsmodi_en.html/c458080 (2019-08-05).
39. M. Rössle, W. Leitenberger, M. Reinhardt, A. Koç, J. Pudell, C. Kwamen, and M. Bargheer, "The time-resolved hard X-ray diffraction endstation KMC-3 XPP at BESSYII," J. Synchrotron Radiat. **28**(3), 948–960 (2021).
40. D. Morgan and E. Paige, *Surface Acoustic Wave Filters (Second edition).*, Studies in Electrical and Electronic Engineering. (Academic Press, Oxford., 2007), 2nd edition. ed.
41. C. Campbell, *Surface Acoustic Wave Devices and Their Signal Processing Applications* (Academic Press, 1989).